

Evaluation of material structure changing after ultrasonic milling of aluminum foam by Computed Tomography (CT)

Janos Liska¹, Zsolt Ferenc Kovács¹, Ladislav Morovic², Ivan Buransky², Marcel Kuruc², Zsolt János Viharos³, Michaela Kritikos²

¹John von Neumann University, GAMF Faculty of Engineering and Computer Science, Dep. of Vehicle Technology, Kecskemét H-6000 Hungary, liska.janos@gamf.uni-neumann.hu; kovacs.zsolt@gamf.uni-neumann.hu

²Slovak University of Technology in Bratislava, Faculty of Materials Science and Technology in Trnava, ladislav.morovic@stuba.sk; ivan.buransky@stuba.sk; kuruc.marcel@stuba.sk; michaela.kritikos@stuba.sk

³Centre of Excellence in Production Informatics and Control, Institute for Computer Science and Control of the Hungarian Academy of Sciences (MTA SZTAKI), H-1111, Kende str. 13-17., Budapest, Hungary, viharos.zsolt@sztaki.mta.hu

Abstract – In our everyday lives, we spend more and more time in our vehicles, where we are exposed to growing accident hazards. That is why we are increasingly focusing on security. This is particularly true for electric cars, where the size of the power source and the firewall are not the same as for conventional vehicles. The so-called energy-absorbing zone has a key role during an accident. In the era of modern materials the aluminum foam can work as an energy-absorbing structure. However, the machining of this material is hard at this time. This article attempts to investigate, through Computed Tomography-CT technology, whether the material has a permanent deformation or dimensional variation in the structure of the material can be achieved by the ultrasonic milling process.

Keywords: Ultrasonic machining, Computer Tomography (CT), Industrial CT, 3D Measurement, Aluminum foam.

I. INTRODUCTION

Recently, several scientific journals dealt with the problems of metal foam machining. Metal foams belong to the group of so-called cellular materials. Currently can create cellular materials from several materials, such as polymers, ceramics, glasses, composites, aluminium, copper, metals or these mixture [1]. Recently, metallic foam has been considered for use as impact energy-absorption material for cars, trains and airplanes to take advantage of its lightweight and unique compression

deformation characteristics [2].

In this study a special type of foam, namely the aluminium alloy foam was investigated. This material has many advantages thanks to the cellular structure. For example, the heat-transfer and impact energy-absorption properties are excellent [1, 3, 4]. But about this good properties the machinability is bad. Haipeng Qiao at al. are investigated the subsurface damage of cells. Based on their results the depth of deformation can reach the 5 mm, see in Fig. 1. [5].

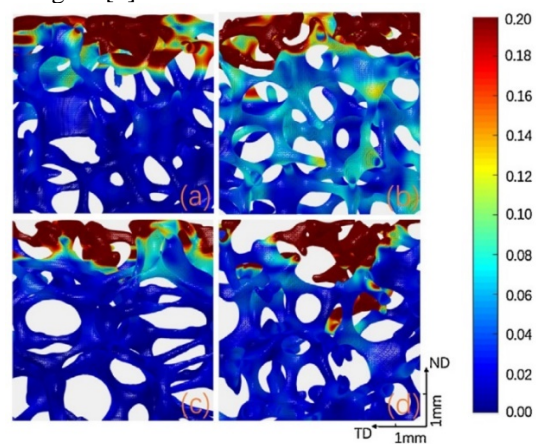


Fig. 1. Subsurface strain field from DVC of samples machined at $vc = 2.6$ m/s, feed rates of (a and c) $vf = 0.102$ mm/min and (b and d) $vf = 0.204$ mm/min, axial depths of cut of (a and b) $ap = 1.5$ mm and (c and d) $ap = 1.0$ mm [5]

The problem of the machinability is that, while a simple aluminium alloy can be machinable with a standard carbide tool, of course which is specially

designed for aluminium, but this tool insert not fit for aluminium foam because of the cellular structure and special alloys contents are require different carbide type and also tool geometry.

This also means problem for the tool manufacturer companies because they need to develop special tools which not only suitable for a particular material type, material properties (e.g. tools for Al machining).

To create this type of special tool we have determine the machinability of aluminium foam by various experiments. However, there are not many methods that can be used, because mostly the aluminium foams contains Al_2O_3 grains and made by air bubbles technology, this means that the workpiece structure is not compact and hollow. It is practically a cellular light structure where the thickness of the walls between the cells is very small (depending on the size of the cells). In this regard, it is hard to machining because there are several accompanying phenomena at the same time. Mainly the very intensive tool wear, negative burr formation, edge burr and damaged cells occurs the problems. These accompanying phenomena also destroy material surface, size and accuracy.

II. RELATED RESULTS IN THE LITERATURE

In order to better understand the causes of the phenomena, we believe that it is necessary to get to know the process of chip formation. In our opinion, ultrasonic high-speed machining technology can be used to minimize, possibly eliminate, the edge burr defect, tribological behaviour, reduce machining force and the subsequent cell destruction [6-8].

For the experiment an ultrasonic vibration assisted milling machine was used (DMG Sauer Ultrasonic 20 linear). It is a five-axis rotary ultrasonic and high-speed cutting machine tool. The ultrasonic tool vibration is generated by a piezo crystal (Fig. 2.), which can vibrate in range 20 to 30 kHz (its value depends on the tool diameter and length of acoustic assembly). High speed cutting is ensured by spindle, which can reach up to 42,000 rpm. Feed rate acceleration is over 2g and its value can reach value 40,000 mm/min.

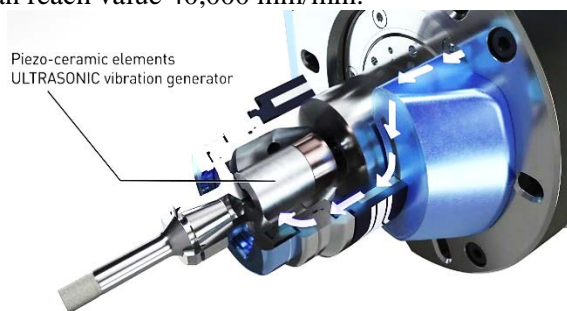


Fig. 2. Principle of ultrasonic milling [9]

This machine tool has a 5-axis gantry construction with an integrated NC swivel rotary table; therefore, it can machine complex shapes in one clamping. Its kinematic scheme is shown in the Fig. 3. The tool performs all three linear movements (X, Y, Z). Range of motions in these axes are: 200 mm in the X axis, 200 mm in the Y axis and 280 mm in the Z axis. Workpiece performs two remaining rotational movements (A, C). Rotation around X axis (A) is ensured by the cradle construction. Movement around this axis is limited by range -10° to $+130^\circ$. Rotation around Z axis (C) is ensured by the rotary table. Movement around this axis is not limited. Velocity of rotational motions could reach the value up to 200 rpm. Performance of the machine is 15 kW. Torque momentum can achieve the value 6 Nm. It has high precision of positioning ($\pm 2.5 \mu m$). The cooling system can supply the process liquid or the pressured air by four outer nozzles and by the core of the tool. The tool magazine has 24 slots for different types of tools. In front of the tool magazine is also the laser measuring device for measuring the tool characteristics (like length and diameter). This machine tool operates under Sinumerik 840 solutionline control system [10, 11].

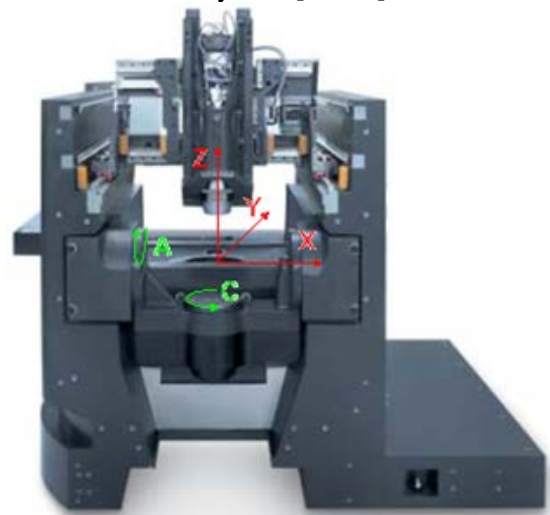


Fig. 3. Kinematic scheme of the controlled axes for DMG Ultrasonic 20 linear [12]

Of course there are other solution for aluminium foam machining for example the chemical milling. This process can produces smooth surfaces without damage but the machining time requirement so high [13, 14].

III. DESCRIPTION OF THE METHOD

As any machining process an experiment is performed, it is necessary to evaluate the data obtained with a design method or software. In this article the authors use the

Taguchi method to evaluate their results.

During of the experiment the parameter of cutting speed, cutting depth and feed per tooth were changed, so were selected as three experimental factors (parameters) and designated as factors A–C (Table 1).

Table 1. Milling conditions

| Parameters | Experimental conditions | | |
|------------------------------------|-------------------------|------|-----|
| | 1 | 2 | 3 |
| A Cutting speed, v_c (m/min) | 400 | 500 | 600 |
| B Cutting depth, a_p (mm) | 2 | 3 | 5 |
| C Feed per tooth, f_z (mm/tooth) | 0,02 | 0,06 | 0,1 |

Three levels for each factor were configured to cover the range of interest and identified by the digits 1, 2, and 3 respectively. The L9 orthogonal array was selected to conduct the matrix (Table 2).

Table 2. Design matrix of the experiment

| Exp. No. | Parameter combinations | | |
|----------|------------------------|---|------|
| | A | B | C |
| 1 | 400 | 1 | 0,02 |
| 2 | 400 | 3 | 0,06 |
| 3 | 400 | 5 | 0,10 |
| 4 | 500 | 3 | 0,02 |
| 5 | 500 | 5 | 0,06 |
| 6 | 500 | 1 | 0,10 |
| 7 | 600 | 5 | 0,02 |
| 8 | 600 | 1 | 0,06 |
| 9 | 600 | 3 | 0,10 |

IV. RESULTS AND DISCUSSIONS

Due to the structure of the aluminium foam the extent of structural changes is not easy because the degree of lesion is not linear in each cross section of the material.

In this respect, before and after the ultrasonic milling industrial Computed Tomography (CT) technology is used. The measuring equipment is an industrial CT, Zeiss Metrotom 1500 (Fig. 4). Specification of the used equipment is in the Table 1.

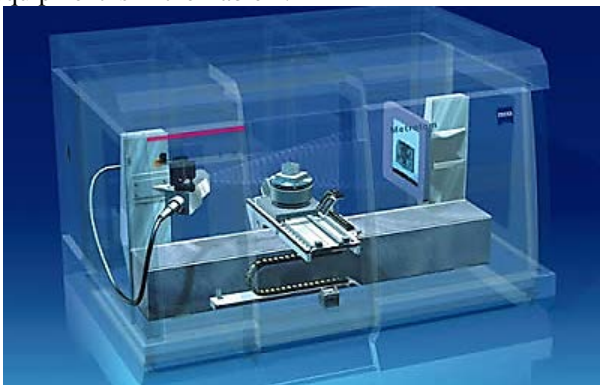


Fig. 4. Zeiss Metrotom 1500 industrial CT [15]

With this equipment it is also possible to examine the internal structure of the material. Our assumption is that, even during cutting directly below the machining zone the cells suffer deformation in the layers [16-18]. Knowledge of this can be important information for future use (e.g. formation of energy-absorbing zones).

Table 3. METROTOM 1500 specification

| | |
|-------------------------------|----------------------|
| Tube power (W) | 500 |
| Tube voltage (kV) | 225 |
| Measuring range (mm) | dia. 350x300 |
| Detector resolution (Pixel) | 1024x1024; 2048x2048 |
| Source/detector distance (mm) | 1500 |
| Tube type | Open X-ray |

This experimental investigation was examined at a distance of 360 mm from X-Ray lamp with voxel size of 98 μ m. Software used for scanning was METROTOM OS 2.8 (Fig. 5).

Integration time was 1000 ms and it was used 1050 pictures for evaluation. It took 45 minutes of scanning. Voltage value was used of 190 kV and current was used 600 μ A.

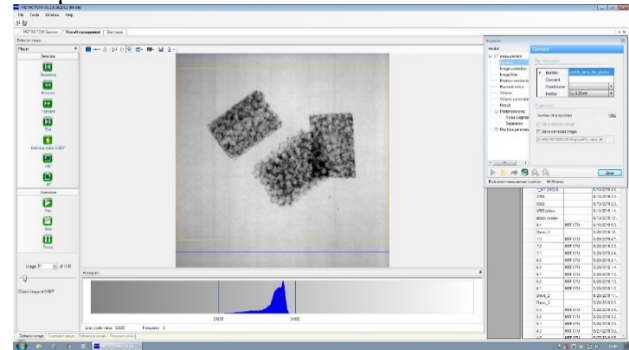


Fig. 5. METROTOM OS 2.8 interface

As it is seen in the figure above 3 pieces were scanned in one measurement. After they were separated and evaluated.

Before and after ultrasonic milling the specimens was 3D digitized by CT. This made it possible to compare the digitized 3D models, which was realized by software GOM ATOS Professional software.

The comparison aimed to determine the change in the geometry of the aluminium foam specimen, which we assume due to the cutting forces and possibly by the specimen clamping. At the beginning of the comparison process, the correct and accurate alignment of both samples is very important. The above mentioned comparison was evaluated respectively visualized by colour deviation map of shapes (and dimensions) (Fig. 6.) as well as by inspection sections in defined locations.

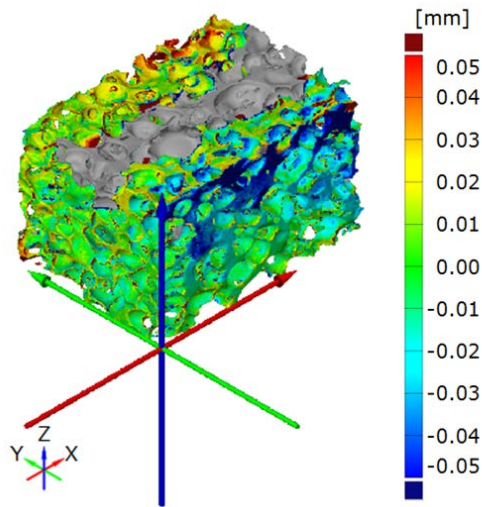


Fig. 6. Colour deviation map of shapes (and dimensions)

For the quantification of deviation evaluation of shapes and dimensions, inspection sections were used. For each comparison, 3 inspection sections were created: 2 inspection sections perpendicular to the X-axis at a distance of 2 mm from the side walls of the specimen and 1 inspection section at the centerline of the specimen along the slot (Fig. 7.).

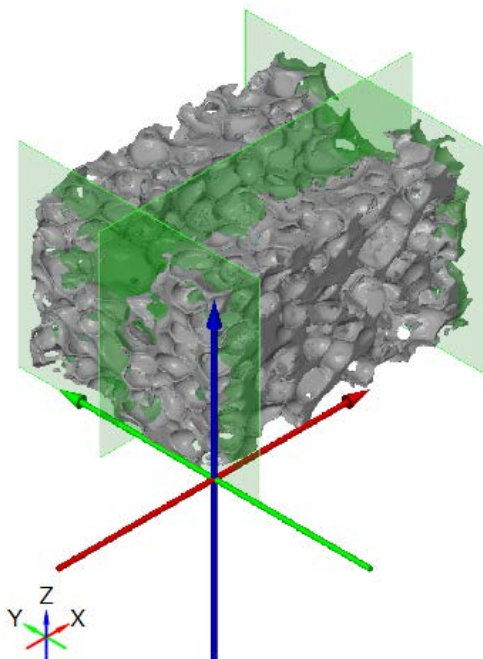


Fig. 7. Positions of the inspection sections

V. CONCLUSIONS

After the CAD comparison we get a surface deviations on the milled surfaces (Fig. 8). This model is very similar to Fig. 5, but here we can see the original part deleted.

The Fig. 8 clearly show the max. and minimum

deviation from the original model. We can see also (on the right side of the model) the deformation of the clamping system. This deformation is not very high, but it is important fact (ho fixing and clamping of the foam materials).

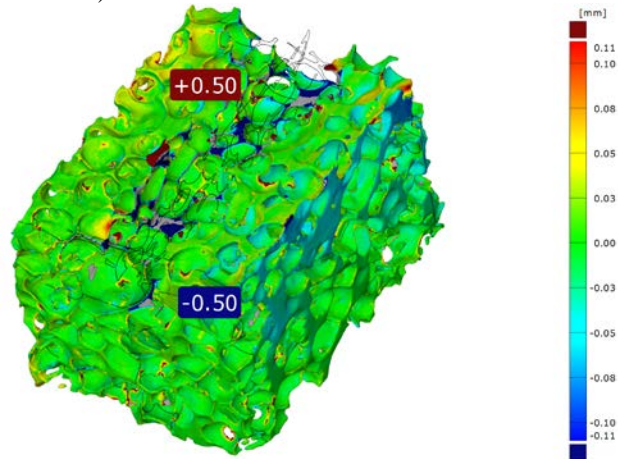


Fig. 8. Result of the milled surface deviations

After the inspection sections (Fig. 7), we can get the section planes from the deformed models (Fig. 9). Here we can see 3 planes. The first was the input, the third was the output of the tool during milling. And we have second also. This section represent across of the toolpath. This section plane was the most important, because here was biggest deformation. It is also very important, under of the milled zone was also cell deformations.

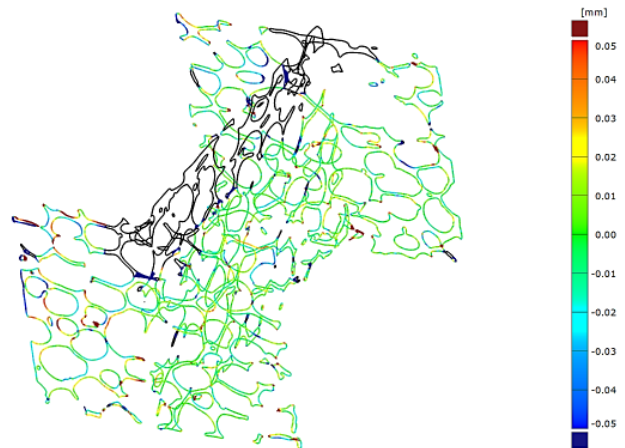


Fig. 9. Deformed parts of the inspection section planes

After the inspection section evaluations we observed the max. and min. deviations in the section planes. By the help of the statistical software we get a regression of the measured values. The regression was very wrong (because the material was very inhomogeneous), but we get some good results. On the base of the regression we can say: the feed per tooth (f_z) was the most important factor of this experiments. The F-significant value was 0,051 and also the p-value have similar number. This factor (f_z) was the only one from the DOE which have

more significant values. On the future we plan make more experiments, and we plane also work out the new measuring method (after cutting) for this type of materials.

VI. ACKNOWLEDGMENTS

This research is party supported by EFOP-3.6.1-16-2016-00006 "The development and enhancement of the research potential at John von Neumann University" project. The Project is supported by the Hungarian Government and co-financed by the European Social Fund.

REFERENCES

- [1] **Guarino, S.; Rubino, G.; Tagliaferri, V.; Ucciardello, N.:** Thermal behavior of open cell aluminum foams in forced air: Experimental analysis, *Measurement*, Vol. 60, 2015, pp. 97–103.
- [2] **Vesenjak, M.; Krstulovic-Opara, L.; Ren, Z.; Öchsner, Z.; Domazet, Z.:** Experimental study of open-cell cellular structures with elastic filler material, *Exp. Mech.*, Vol 49, 2009, pp. 501–509.
- [3] **Beer, M.; Rybár, R.; Kal'avsky, M.:** Experimental heat transfer analysis of open cell hollow ligament metal foam at low Reynolds number, *Measurement*, Vol. 133, 2019, pp. 214–221.
- [4] **Tanaka, S; Hokamoto K.; Irie, S.; Okano, T.; Ren, Z.; Vesenjak, M.; Itoh, S.:** High-velocity impact experiment of aluminum foam sample using powder gun, *Measurement*, Vol. 44, 2011, pp. 2185-2189.
- [5] **Qiao, H.; Basu, S.; Saladana, C.; Kumara, S.:** Subsurface damage in milling of lightweight open-cell aluminium foams, *CIRP Annals - Manufacturing Technology*, Vol. 66, Issue 1, 2017, pp. 125-128.
- [6] **Xing, D.; Zhang, J.; Shen, X.; Zhao, Y.; Wang, T.:** Tribological properties of ultrasonic vibration assisted millingaluminium alloy surfaces, *Procedia CIRP*, Vol. 6, 2013, pp. 539-544.
- [7] **Ni, C.; Zhu, L.; Liu, C.; Yang, Z.:** Analytical modeling of tool-workpiece contact rate and experimental study in ultrasonic vibration-assisted milling of Ti-6Al-4V, *International Journal of Mechanical Sciences*, Vol. 142-143, 2018, pp. 97-111.
- [8] **Verma, G. C.; Pandey, P. M.:** Machining forces in ultrasonic-vibration assisted end milling, *Ultrasonics*, Vol 94, 2019, pp. 350-363.
- [9] <https://images.app.goo.gl/da4jz9tRhvuKbbhN8> (01.05.2019)
- [10] **Kuruc, M.; Zvončan, M.; Peterka, J.:** Investigation of ultrasonic assisted milling of aluminum alloy AIMg4.5Mn. In *Procedia Engineering*, vol. 69 (2014), pp. 1048 - 1053, 24th DAAAM International Symposium on Intelligent Manufacturing and Automation, <https://www.sciencedirect.com/science/article/pii/S187770581400335X>, (01.05.2019).
- [11] **Kuruc, M.; Zvončan, M.; Peterka, J.:** Comparison of conventional milling and milling assisted by ultrasound of aluminum alloy AW 5083. In *IN-TECH 2013: Proceedings of International Conference on Innovative Technologies*, Budapest, Hungary, 2013. Rijeka: Faculty of Engineering University of Rijeka, 2013, pp.177-180. ISBN 978-953-6326-88-4.
- [12] DMG Ultrasonic 20 linear. <https://en.dmgmori.com/products/machines/ultrasonic/ultrasonic-linear>, (01.05.2019)
- [13] **Matsumoto, Y.; Brothers, A.H.; Stock, S.R.; Dunand, D.C.:** Uniform and graded chemical milling of aluminum foams, *Materials Science and Engineering*, Vol. 447, 2007, pp. 150-157.
- [14] **Li, Q.; Wang, J.; Hu, W.:** Optimizations of electric current assisted chemical milling condition of 2219 aluminum alloy, *Journal of Materials Processing Tech.*, Vol. 249, 2017, pp. 379-385.
- [15] **Plastic Fantastic:** Carl Zeiss Metrotom 1500 industrial CT scanner <http://plasticszone.blogspot.com/2008/09/carl-zeiss-metrotom-1500-industrial-ct.html>, (01.05.2019)
- [16] **Tian, W.; Han, N.:** Analysis on meso-damage processes in concrete by X-ray computed tomographic scanning techniques based on divisional zones, *Measurement*, Vol. 140, 2019, pp. 382–387.
- [17] **Hiller, J.; Reindl, L. M.:** A computer simulation platform for the estimation of measurement uncertainties in dimensional X-ray computed tomography, *Measurement*, Vol. 45, 2012, pp. 2166–2182.
- [18] **Chen, S-W.; Chu, C-Y.:** A comparison of 3D cone-beam Computed Tomography (CT) image reconstruction performance on homogeneous multi-core processor and on other processors, *Measurement*, Vol. 44, 2011, pp. 2035–2042.